Communications in Information and Systems
Volume 19, Number 4, 391–403, 2019

Machine learning of the rate constants for the reaction between alkanes and hydrogen/oxygen atom

Junhui Lu[†,‡,¶], Jinhui Yu[†,‡,¶], Hongwei Song[†], and Minghui Yang[†,‡,§,*]

The reaction rate constant is critical in modeling combustion and biochemistry reaction network. In this work, a machine learning approach using multi-layered neural network (NN) models is applied to training and predicting rate constants of combustions reactions. Two kinds of hydrogen abstraction reactions are considered: Hydrogen + Alkanes (HR) and Oxygen + Alkanes (OR). Each reaction is described by five parameters: three of which distinguish the structure of the reactant alkane, one is the serial number of the carbon atom for the broken C-H bond and the last one is the temperature. Two NN models are trained separately by fitting the rate constants of eight HR or eleven OR reactions. The small deviations indicate that the rate constants can be well represented by the NN models. To test the predictive ability, one model is constructed for each reaction by fitting the rates constants of the rest n-1 reactions ($n = 8$ for HR reactions and $n = 11$ for OR reactions). The deviations are 25.3%-2396.3% for the HR reactions and 15.0%-659.4% for the OR reactions. Most of the prediction results are better than those from the transition state theory. Overall, the machine learning approach is an efficient method to predict chemical reaction rate constants.

Keywords and phrases: Machine learning, neural network, rate constant, alkane.

*The corresponding author.

[†]Key Laboratory of Magnetic Resonance in Biological Systems, State Key Laboratory of Magnetic Resonance and Atomic and Molecular Physics, National Center for Magnetic Resonance in Wuhan, Wuhan Institute of Physics and Mathematics, Chinese Academy of Sciences, Wuhan 430071, China.

[‡]University of Chinese Academy of Sciences, Beijing 100049, China.

[§]Wuhan National Laboratory for Optoelectronics, Huazhong University of Science and Technology, Wuhan 430071, China.

[¶]These authors contributed equally to this work.

1. Introduction

The reaction rate constant is a fundamental quantity of chemical reaction and plays an important role in modeling combustion and biochemistry reaction network. The accurate determination of thermal rate constants for chemical reactions is one of the major objectives of experimental and theoretical chemistry [1]. Experimentally, the thermal rate constant can be measured by discharge flow, flash photolysis, shock tube, laser induced fluorescence and other techniques [2, 3]. Theoretically, the reaction rate constants could be calculated using the transition state theory (TST) [4, 5] or chemical dynamics methods, such as quasi-classical trajectory method [6], multi-configuration time-dependent Hartree method [7], ring polymer molecular dynamics method [8] and time-dependent wave-packet method [9]. The chemical dynamics calculation demands a pre-build potential energy surface and the costs of computations are relatively high. Nowadays, most of the measured or computed rate constants are available on the website of National Institute of Standards and Technology (NIST, https://www.nist.gov/).

Recently, machine learning is becoming a powerful tool in the field of theoretical and computational chemistry. Zare and co-workers developed a model called the Deep Reaction Optimizer to guide the interactive decision-making procedure in optimizing reactions by combining state-of-the-art deep reinforcement learning with the domain knowledge of chemistry [10]. Coley *et al.* used a machine learning method to predict organic reaction outcomes [11]. Lately, machine learning was applied to predicting the reaction rate constants. Zhong *et al.* combined Deep Neural Network with Molecular Fingerprints to develop models to predict ·OH radical rate constants of 593 organic contaminants [12]. Bowman and co-workers reported a machine learning approach to train and predict bimolecular thermal rate constants over a wide range of temperatures [1].

The chemical reactions usually have the same mechanism if their reactants are of similar structures. Therefore, we attempt to predict the rate constants of alkanes with oxygen/hydrogen by using neural network (NN) models with the same descriptors. This work is organized as follows. Section 2 introduces the descriptor and the machine learning approach employed. In the third section, the results and discussions are presented. Finally, we make a conclusion in Section 4.

2. Methods

2.1. Descriptors

In this work, two kinds of hydrogen abstract reactions are studied, which are listed below:

(R1) $$C_nH_{2n+2} + H \rightarrow C_nH_{2n+1} + H_2$$

(R2) $$C_nH_{2n+2} + O \rightarrow C_nH_{2n+1} + OH$$

To characterize these reactions, five parameters are used: three of them are the topological indices for the molecular structure of the reactant Alkane, one is the serial number of the carbon atom for the broken C-H bond and the last one is the temperature.

The three topological indices (denoted as $ND_1/ND_2/ND_3$) are calculated as follows [13]:

2.1.1. Distance matrix A bidimensional $(n \times n)$ distance matrix is defined by (n is the number of non-hydrogen atoms in the molecule):

$$D_m = (d_{ij})_m = \begin{cases} m, & \text{the number of C-C bond(s) between } C_j \text{ and } C_i \text{ atom} = m \\ 0, & \text{the number of C-C bond(s) between } C_j \text{ and } C_i \text{ atom} \neq m \end{cases}$$

2.1.2. Branching degree The properties of isomers vary with the branching degree, which can be calculated by:

(1) $$g_i = \left(\sum k\right)^{0.5}$$

The g_i means the branching degree of the i-th carbon atom, $\sum k$ represents the sum of the number of the single bonds between the i-th atom and other non-Hydrogen atoms.

2.1.3. Equilibrium electronegativity The strength of the bond is closely related to the electronegativity of the bonding atoms. The electronegativity of the atoms varies with their chemical environment. The equilibrium electronegativity of the i-th atom in the molecule is defined by:

(2) $$\chi_i = \frac{(\chi_{iA} + \sum \chi_G)}{(1 + \sum l)}$$

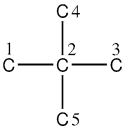

Figure 1: Hydrogen-suppressed graph of 2,2-Dimethylpropane.

where

$$\chi_G = \left\{ \frac{1}{n_{1l}} \sum_{l=1}^{n_{1l}} \left[\frac{1}{n_{2l}} \sum_{l=1}^{n_{2l}} \left(\frac{1}{n_{il}} \sum_{l=1}^{n_{il}} \chi_{il} \right) \right] \right\} \tag{3}$$

and $\chi_{i\mathrm{A}}$ is the Pauling electronegativity, $\sum \chi_G$ is the sum of equilibrium electronegativity of atoms connected to the i-th atom, $\sum l$ is the total number of radicals connected with i-th atom.

2.1.4. Augmented distance matrix The augmented distance matrix Q_m is obtained by combining the vectors $\{\mathrm{g}_i\}$, $\{(\chi_i)^{0.5}\}$ and the matrix $Q_m(m{=}1,2,3)$. The vectors $\{\mathrm{g}_i\}$ and $\{(\chi_i)^{0.5}\}$ are placed in the first and second columns, respectively. For example, the augmented distance matrices Q_1, Q_2 and Q_3 of 2,2-Dimethylpropane, as shown in Figure 1, are

$$Q_{\mathbf{1}} = \begin{bmatrix} 1 & 1.5168 & 0 & 1 & 0 & 0 & 0 \\ 2 & 1.5297 & 1 & 0 & 1 & 1 & 1 \\ 1 & 1.5168 & 0 & 1 & 0 & 0 & 0 \\ 1 & 1.5168 & 0 & 1 & 0 & 0 & 0 \\ 1 & 1.5168 & 0 & 1 & 0 & 0 & 0 \end{bmatrix}$$

$$Q_{\mathbf{2}} = \begin{bmatrix} 1 & 1.5168 & 0 & 0 & 2 & 2 & 2 \\ 2 & 1.5297 & 0 & 0 & 0 & 0 & 0 \\ 1 & 1.5168 & 2 & 0 & 0 & 2 & 2 \\ 1 & 1.5168 & 2 & 0 & 2 & 0 & 2 \\ 1 & 1.5168 & 2 & 0 & 2 & 2 & 0 \end{bmatrix}$$

$$Q_{\mathbf{3}} = \begin{bmatrix} 1 & 1.5168 & 0 & 0 & 0 & 0 & 0 \\ 2 & 1.5297 & 0 & 0 & 0 & 0 & 0 \\ 1 & 1.5168 & 0 & 0 & 0 & 0 & 0 \\ 1 & 1.5168 & 0 & 0 & 0 & 0 & 0 \\ 1 & 1.5168 & 0 & 0 & 0 & 0 & 0 \end{bmatrix}$$

Table 1: The *ND* indices of all alkanes collected

Alkane	ND_1	ND_2	ND_3
CH_4	2.2701	2.2701	2.2701
C_2H_6	7.5747	6.5747	6.5747
C_3H_8	12.8170	13.5618	10.8170
n-C_4H_{10}	17.6688	19.1027	20.3096
n-C_5H_{12}	22.2959	25.8268	26.9664
n-C_6H_{14}	26.8086	31.6892	32.7079
iso-C_4H_{10}	17.9683	28.0449	14.9683
iso-C_5H_{12}	22.5862	31.5720	31.9442
neo-C_5H_{12}	23.0683	50.8790	19.0683

2.1.5. *ND* indices The topological indices are calculated by:

$$\begin{aligned} M_{\mathbf{1}} &= Q_{\mathbf{1}} \times {Q_{\mathbf{1}}}^{\mathrm{T}} \\ M_{\mathbf{2}} &= Q_{\mathbf{2}} \times {Q_{\mathbf{2}}}^{\mathrm{T}} \\ M_{\mathbf{3}} &= Q_{\mathbf{3}} \times {Q_{\mathbf{3}}}^{\mathrm{T}} \\ ND_1 &= \lambda_{\max 1} \\ ND_2 &= \lambda_{\max 2} \\ ND_3 &= \lambda_{\max 3} \end{aligned} \tag{4}$$

in which $\lambda_{\max 1}$, $\lambda_{\max 2}$ and $\lambda_{\max 3}$ are the maximum eigenvalues of M_1, M_2 and M_3, respectively. The $ND_1/ND_2/ND_3$ indices of 2,2-Dimethylpropane are 23.0683/50.8790/19.0683. All alkanes involving no more than twelve C atoms can be uniquely determined in a three-dimensional space by the three indices [13].

The products are distinguished by a rule similar to the IUPAC rules [14], where the carbon atoms in the principal and side chains are ordered serially. In this work, the product is coded according to the carbon atom of the broken C-H bond. The parameters $ND_1/ND_2/ND_3$ for the reactants are listed in Table 1.

2.2. Neural network models

The NN models are trained under the framework of PyTorch [15] by fitting rate constants. The NN models consist of 1 input layer with aforementioned five parameters, 3 hidden layers with 100 neurons in each layer and 1 output layer. The Mean Square Error (MSE) Loss function and Adam optimizer are used during the process of model training. The learning rate is 1E-4 and the

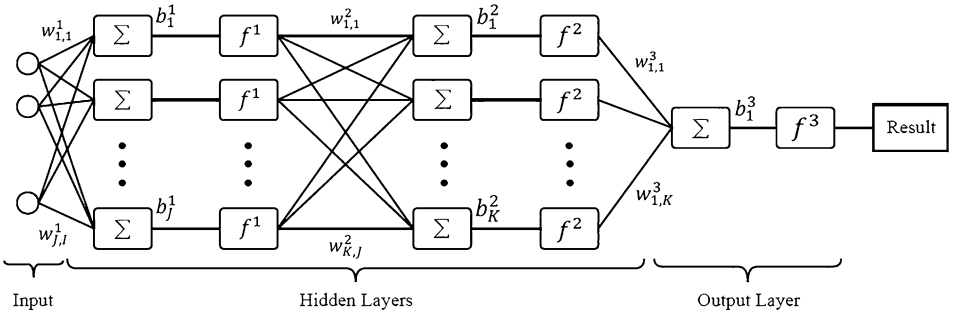

Figure 2: The schematic diagram of the neural network. $w_{j,i}$: the connection weight between the i-th neuron of the input layer and the j-th neuron of the first hidden layer; b_j: the bias of j-th neuron of the first hidden layer; f: the activation function.

batch size is 1. Here, the root mean square (RMS) error is used to evaluate the performance of the developed models. Figure 2 shows the schematic diagram of the neural network (taking two hidden layers of neurons as an example).

3. Results and discussion

In this work, the rate constants of the eight HR reactions and eleven OR reactions, as listed in Table 2, are firstly collected from the NIST Chemical Kinetics Database. However, the rate constants available in the NIST database are very limited due to the difficulty of experimental measurements. It has been generally recognized that the prediction accuracy of neural network models is guaranteed by enough data. Hence, more rate constants are obtained by the three-parameter Arrhenius equation,

$$k(T) = AT^n e^{-E/RT} \tag{5}$$

in which the parameters A, n, and E are determined by fitting the experimental rate constants. T is the temperature and R is the molar gas constant. Finally, a total of 2186 values are used for the eight Alkane + Hydrogen reactions at the temperatures ranging from 230 K to 2500 K and 3339 values are used for the eleven Alkane + Oxygen reactions in the temperature range from 250 K to 2500 K. Since the rate constant k ranges from 10^{-18} to 10^{-19}, $\log k(T)$ is used in the calculations.

Table 2: List of reaction channels considered in this work

Reaction type	Reaction number	Reaction channel	Reference
Alkane + H	HR1	$CH_4 + H \rightarrow H_2 + CH_3$	[16]
	HR2	$C_2H_6 + H \rightarrow H_2 + C_2H_5$	[17]
	HR3	$C_3H_8 + H \rightarrow H_2 + n\text{-}C_3H_7$	[18]
	HR4	$C_3H_8 + H \rightarrow H_2 + iso\text{-}C_3H_7$	[18]
	HR5	$n\text{-}C_4H_{10} + H \rightarrow H_2 + sec\text{-}C_4H_9$	[19]
	HR6	$iso\text{-}C_4H_{10} + H \rightarrow H_2 + iso\text{-}C_4H_9$	[20]
	HR7	$iso\text{-}C_4H_{10} + H \rightarrow H_2 + tert\text{-}C_4H_9$	[20]
	HR8	$neo\text{-}C_5H_{12} + H \rightarrow H_2 + (CH_3)_3CCH_2$	[21]
Alkane + O	OR1	$CH_4 + O \rightarrow CH_3 + OH$	[17]
	OR2	$C_2H_6 + O \rightarrow C_2H_5 + OH$	[17]
	OR3	$C_3H_8 + O \rightarrow n\text{-}C_3H_7 + OH$	[18]
	OR4	$C_3H_8 + O \rightarrow iso\text{-}C_3H_7 + OH$	[18]
	OR5	$n\text{-}C_4H_{10} + O \rightarrow n\text{-}C_4H_9 + OH$	[22]
	OR6	$n\text{-}C_4H_{10} + O \rightarrow sec\text{-}C_4H_9 + OH$	[22]
	OR7	$iso\text{-}C_4H_{10} + O \rightarrow iso\text{-}C_4H_9 + OH$	[20]
	OR8	$iso\text{-}C_4H_{10} + O \rightarrow tert\text{-}C_4H_9 + OH$	[20]
	OR9	$n\text{-}C_5H_{12} + O \rightarrow 1\text{-}C_5H_{11} + OH$	[22]
	OR10	$n\text{-}C_5H_{12} + O \rightarrow CH_3CH_2CH_2CHCH_3 + OH$	[22]
	OR11	$neo\text{-}C_5H_{12} + O \rightarrow (CH_3)_3CCH_2 + OH$	[23]

3.1. Models training and validation

The data is randomly divided into two parts: a training set (80%) and a validation set (20%). The RMS value is defined as [1]:

$$RMS_i = \left(\left(\frac{1}{j\max}\right)\left(\sum_{j=1}^{n} log_{10}\left(\frac{k_{fit}}{k_{exp}}\right)_i^2\right)\right)^{\frac{1}{2}} \tag{6}$$

where k_{exp} is the sampled rate constants, k_{fit} is the corresponding fitted or predicted rate constants, i refers to one of the reactions listed in Table 2, and n is the number of sampled rate constants for the i-th reaction in the training set or the validation set. The average deviation δ_i is calculated by:

$$\delta_i = 10^{RMS_i}\text{-}1 \tag{7}$$

Four kinds of models are constructed, for which 1, 2, 3 and 4 hidden layers (labeled as L1, L2, L3 and L4 model) are included with 100 neurons

Table 3: The RMSs and deviations of the validation set for different models. n in L_n denotes the number of hidden layers included in the model

Model type	HR			OR		
	RMS	Deviation	Time	RMS	Deviation	Time
L1	0.3157	106.9%	1	0.1528	42.2%	1
L2	0.0729	18.3%	1.4	0.0656	16.3%	1.4
L3	0.0343	8.2%	2	0.0231	5.5%	2
L4	0.0276	6.6%	2.4	0.0505	12.3%	2.4

in each hidden layer. The RMSs and deviations of these models are shown in Table 3. The deviations of the L1 and L2 models are large while the deviations of the L3 and L4 models are relatively small. However, as the number of the hidden layer increases, the training becomes difficult. To balance the computational accuracy and efficiency, the L3 model is employed hereafter. Therefore, two NN models with the same architecture as the L3 model are constructed separately for the Hydrogen + Alkane (HR) and Oxygen + Alkane (OR) reactions.

For HR reactions, the RMS values for the training set and validation set are 0.0375 and 0.0343, respectively. The corresponding average deviations are 9.0% and 8.2%. For OR reactions, the RMS values for the training set and validation set are 0.0359 and 0.0231, respectively. The corresponding deviations are 8.6% and 5.5%. Since the number of sampled data points for OR reactions is larger than that of HR reactions, the RMS for OR reactions is smaller. Overall, the small values of RMSs for the two kinds of reactions indicate that the NN models used in this work could represent effectively their rate constants.

3.2. The prediction of rate constants

In this subsection, the predictive ability of the NN models is explored. The architecture of the NN models is the same as the L3 model. However, only (n-1) reactions are involved in the training and the rest one is used for prediction. For each reaction, ten NN models are trained using the data of the other reactions and the model with the smallest RMS is used in the following discussions.

Houston *et al.* [1] suggested that the predictive ability can be divided into three levels: "accurate" means a deviation smaller than 100%; "reasonable" refers to a deviation of about 300% since the averaged deviation calculated by the TST is approximately 300%; and "inaccurate" denotes a deviation larger than 500%. The RMSs and deviations for HR reactions are listed in

Table 4: The RMSs and deviations of predicted rate constants for Alkanes + Hydrogen

Reaction number	RMS	Deviation
HR1	0.9772	848.8%
HR2	0.157	43.6%
HR3	0.4789	201.2%
HR4	0.0979	25.3%
HR5	0.5492	254.1%
HR6	0.5867	286.1%
HR7	0.7451	456.1%
HR8	1.3973	2396.3%

Table 4. The predictions are accurate for HR2 and HR4 as their deviations are less than 50%, reasonable for HR3, HR5, HR6 and HR7, and inaccurate for HR1 and HR8. The deviations for HR1 and HR8 are 848.8% and 2396.3%, respectively. The poor performance of the NN models for HR1 and HR8 is possibly caused by the inability of the descriptors. The topological indices ($ND_1/ND_2/ND_3$) for the two reactions differ remarkably from the others and the characters of the reactants are not included in the training data. The three ND indices are the same for HR1 while they are significantly different from each other for HR8 (see Table 1). It is thus desirable to develop efficacious descriptors in the future.

Table 5 shows the RMSs and deviations for OR reactions. Clearly, the predictions for OR reactions are better than those of HR reactions. As shown in Table 5, the predictions are accurate for the four reactions OR6/8/9/10 and reasonable for the five reactions OR3/4/5/7/11. The deviations for OR1

Table 5: The RMSs and deviations of predicted rate constants for Alkanes + Oxygen

Reaction number	RMS	Deviation
OR1	0.8805	659.4%
OR2	0.7821	505.5%
OR3	0.4369	173.5%
OR4	0.3062	102.4%
OR5	0.3556	126.8%
OR6	0.0942	24.2%
OR7	0.3301	113.9%
OR8	0.1291	34.6%
OR9	0.0922	23.7%
OR10	0.0608	15.0%
OR11	0.4093	156.7%

Table 6: The averaged RMSs and deviations of OR1/OR3

Reaction number	RMS	Deviation	RMS (AVG)	Deviation (AVG)
OR1	0.8805	659.4%	0.7111	414.1%
OR3	0.4369	173.5%	0.1218	32.4%

and OR2 are larger than 500% and the predictions are thought to be inaccurate. These results indicate that machine learning is an efficient tool to predict rate constants of chemical reactions that are difficult to be obtained by experimental measurements or theoretical calculations.

The so-called ensemble approach is widely employed to minimize random errors, in which the accuracy of predictions is improved by multi-model averaging. Here we choose the OR1 and OR3 reactions as examples to test the multi-model averaging approach (Table 6). Ten NN models are constructed for each of the OR1 and OR3 reactions and three of them with the smallest RMSs are averaged for predictions. For the OR1 reaction, the non-averaged RMS is 0.8805 while the average value is 0.7111. The corresponding deviations are 659.4% and 414.1%. For the OR3 reaction, the non-averaged RMS is 0.4369 while the average value is 0.1218. The corresponding deviations are 173.5% and 32.4%, respectively. The multi-model averaging approach is also tested for the other reactions and the predictions are improved as well.

4. Conclusions

This work presents a machine learning approach to train and predict the rate constants of two kinds of fundamental chemical reactions: Alkane + Hydrogen (HR) and Alkane + Oxygen (OR). The rate constants collected in the NIST database (eight HR reactions and eleven OR reactions) and from the fitted three-parameter Arrhenius equation are used in the machine learning. The NN models contain 3 hidden layers with 100 neurons in each layer, which are trained separately for the HR and OR reactions. The input layer includes 5 parameters. The small deviations between the fitted rate constants and the experimental data indicate that the NN model is suitable for describing the rate constants of these reactions.

To test the accuracy of predictions, the NN model is first trained by the rate constants of (n-1) reactions for either HR or OR reactions and then applied to predict the rate constants of the rest one. The deviations are smaller than 300% for most of the reactions, which are close to those from transition state theory. Furthermore, the deviation could be visibly reduced by the multi-model averaging approach.

Acknowledgements

This work is supported by the National Natural Science Foundation of China (Grant No. 21773297 and 21973108 to MY, 21603266 and 21973109 to HS).

References

[1] PL Houston, A Nandi, JM Bowman. A Machine Learning Approach for Prediction of Rate Constants. *J. Phys. Chem. Lett.* **10** (2019), 5250–5258. doi:10.1021/acs.jpclett.9b01810

[2] R Atkinson. Kinetics and Mechanisms of the Gas-Phase Reactions of the Hydroxyl Radical with Organic Compounds under Atmospheric Conditions. *Chem. Rev.* **86** (1986), 69–201. doi:10.1021/cr00071a004

[3] R Atkinson. Kinetics of the Gas-Phase Reactions of OH Radicals with Alkanes and Cycloalkanes. *Atmos. Chem. Phys.* **3** (2003), 2233–2307. doi:10.5194/acp-3-2233-2003

[4] JC Corchado, YY Chuang, PL Fast, W Hu, Y Liu, G Lynch, et al. POLYRATE, version 9.7. University of Minnesota, Minneapolis; (2007). https://comp.chem.umn.edu/polyrate/

[5] JL Bao, DG Truhlar. Variational Transition State Theory: Theoretical Framework and Recent Developments. *Chem. Soc. Rev.* **46** (2017), 7548–7596. doi:10.1039/C7CS00602K

[6] WL Hase, RJ Duchovic, X Hu, A Komornicki, KF Lim, DH Lu, et al. VENUS96: A General Chemical Dynamics Computer Program. *Q.C.P.E. Bulletin.* **16** (1996), 43. https://cdssim.chem.ttu.edu/htmlpages/licensemenu.jsp

[7] U Manthe. A Multilayer Multiconfigurational Time-dependent Hartree Approach for Quantum Dynamics on General Potential Energy Surfaces. *J. Chem. Phys.* **128** (2008), 164116. doi:10.1063/1.2902982

[8] S Habershon, DE Manolopoulos, TE Markland, TF Miller. Ring-Polymer Molecular Dynamics: Quantum Effects in Chemical Dynamics from Classical Trajectories in an Extended Phase Space. *Annu. Rev. Phys. Chem.* **64** (2013), 387–413. doi:10.1146/annurev-physchem-040412-110122

[9] JZH Zhang. *Theory and Application of Quantum Molecular Dynamics.* World Scientific; (1999). doi:10.1142/3713

[10] Z Zhou, X Li, RN Zare. Optimizing Chemical Reactions with Deep Reinforcement Learning. *ACS Central. Sci.* **3** (2017), 1337–1344. doi:10.1021/acscentsci.7b00492

[11] CW Coley, R Barzilay, TS Jaakkola, WH Green, KF Jensen. Prediction of Organic Reaction Outcomes Using Machine Learning. *ACS Central. Sci.* **3** (2017), 434–443. doi:10.1021/acscentsci.7b00064

[12] S Zhong, J Hu, X Fan, X Yu, H Zhang. A deep neural network combined with molecular fingerprints (DNN-MF) to develop predictive models for hydroxyl radical rate constants of water contaminants. *J. Hazard. Mater.* **383** (2020), 121141. doi:10.1016/j.jhazmat.2019.121141

[13] CM Nie, YM Dai, SN Wen, HZ Li. Quantitative Structure-property Relationships for Critical Parameters of Alkane Series. *J. Wuhan Univ. Technol.* **27** (2005), 1–4. https://www.researchgate.net/publication/296728334

[14] S Skonieczny. The IUPAC Rules for Naming Organic Molecules. *J. Chem. Educ.* **83** (2006), 1633. doi:10.1021/ed083p1633

[15] A Paszke, S Gross, S Chintala, G Chanan, E Yang, Z DeVito, et al. Automatic Differentiation in PyTorch; (2017). https://pytorch.org/

[16] JW Sutherland, MC Su, JV Michael. Rate Constants for H+CH_4, CH_3+H_2, and CH_4 Dissociation at High Temperature. *Int. J. Chem. Kinet.* **33** (2001), 669–684. doi:10.1002/kin.1064

[17] DL Baulch, CJ Cobos, RA Cox, C Esser, P Frank, T Just, et al. Evaluated Kinetic Data for Combustion Modelling. *J. Phys. Chem. Ref. Data* **21** (1992), 411–734. doi:10.1063/1.555908

[18] W Tsang. Chemical Kinetic Data Base for Combustion Chemistry. Part 3: Propane. *J. Phys. Chem. Ref. Data.* **17** (1988), 887–951. doi:10.1063/1.555806

[19] RR Baker, RR Baldwin, RW Walker. The Use of the H_2+O_2 Reaction in Determining the Velocity Constants of Elementary Reaction in Hydrocarbon Oxidation. *Symp. Combust. Proc.* **13** (1971), 291–299. doi:10.1016/S0082-0784(71)80032-2 doi:10.1016/S0082-0784(71)80032-2

[20] W Tsang. Chemical Kinetic Data Base for Combustion Chemistry Part 4. Isobutane. *J. Phys. Chem. Ref. Data.* **19** (1990), 1–68. doi:10.1063/1.555877

[21] E Furimsky, KJ Laidler. Kinetics of the Mercury-Photosensitized Decomposition of Neopentane. Part I. The Overall Mechanism. *Can. J. Chem.* **50** (1972), 1115–1122. doi:10.1139/v72-177

[22] N Cohen, KR Westberg. The Use of Transition-State Theory to Extrapolate Rate Coefficients for Reactions of O-Atoms with Alkanes. *Int. J. Chem. Kinet.* **18** (1986), 99–140. doi:10.1002/kin.550180109

[23] N Cohen, KR Westberg. Chemical Kinetic Data Sheets for High-Temperature Reactions. Part II. *J. Phys. Chem. Ref. Data* **20** (1991), 1211–1311. doi:10.1063/1.555901

Junhui Lu
West No. 30 Xiao Hong Shan
Wuhan 430071
China
E-mail address: lujunhui@wipm.ac.cn

Jinhui Yu
West No. 30 Xiao Hong Shan
Wuhan 430071
China
E-mail address: jinhuiyu@wipm.ac.cn

Hongwei Song
West No. 30 Xiao Hong Shan
Wuhan 430071
China
E-mail address: hwsong@wipm.ac.cn

Minghui Yang
West No. 30 Xiao Hong Shan
Wuhan 430071
China
E-mail address: yangmh@wipm.ac.cn
URL: http://tcc.wipm.ac.cn

Received September 30, 2019